AD-A164 167 INDUCED RESONANCE ELECTRON CYCLOTRON (IREC) QUASI-OPTICAL MASER(U) NAVAL RESEARCH LAB WASHINGTON DC P SPRANGLE ET AL 31 JAN 86 NRL-MR-5678 1/1

UNCLASSIFIED F/G 20/5 NL

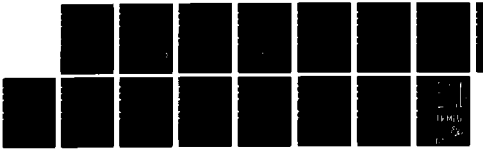

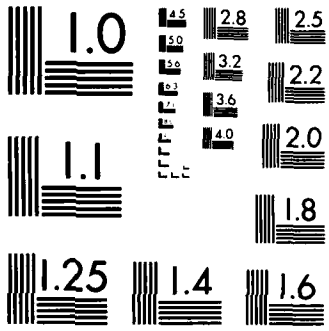

MICROCOPY RESOLUTION TEST CHART

(2)

NRL Memorandum Report 5678

Induced Resonance Electron Cyclotron (IREC) Quasi-Optical Maser

P. SPRANGLE, CHA-MEI TANG AND P. SERAFIM*

Plasma Theory Branch
Plasma Physics Division

**Northeastern University*
Boston, MA 02115

January 31, 1986

This work is supported by the Defense Advanced Research Projects Agency
under Contract No. 5483.

NAVAL RESEARCH LABORATORY
Washington, D.C.

SECURITY CLASSIFICATION OF THIS PAGE

REPORT DOCUMENTATION PAGE

1a. REPORT SECURITY CLASSIFICATION UNCLASSIFIED	1b. RESTRICTIVE MARKINGS
2a. SECURITY CLASSIFICATION AUTHORITY	3. DISTRIBUTION / AVAILABILITY OF REPORT
2b. DECLASSIFICATION / DOWNGRADING SCHEDULE	Approved for public release; distribution unlimited.
4. PERFORMING ORGANIZATION REPORT NUMBER(S) NRL Memorandum Report 5678	5. MONITORING ORGANIZATION REPORT NUMBER(S)
6a. NAME OF PERFORMING ORGANIZATION Naval Research Laboratory 6b. OFFICE SYMBOL (If applicable) Code 4790	7a. NAME OF MONITORING ORGANIZATION
6c. ADDRESS (City, State, and ZIP Code) Washington, DC 20375-5000	7b. ADDRESS (City, State, and ZIP Code)
8a. NAME OF FUNDING / SPONSORING ORGANIZATION DARPA 8b. OFFICE SYMBOL (If applicable)	9. PROCUREMENT INSTRUMENT IDENTIFICATION NUMBER
8c. ADDRESS (City, State, and ZIP Code) Arlington, VA 22209	10. SOURCE OF FUNDING NUMBERS PROGRAM ELEMENT NO. 62702E; PROJECT NO. 5483; TASK NO.; WORK UNIT ACCESSION NO. DN155-384

11. TITLE (Include Security Classification)

Induced Resonance Electron Cyclotron (IREC) Quasi-Optical Maser

12. PERSONAL AUTHOR(S)
Sprangle, P., Tang, Cha-Mei and Serafim, P.*

13a. TYPE OF REPORT	13b. TIME COVERED	14. DATE OF REPORT (Year, Month, Day)	15. PAGE COUNT
Interim	FROM _____ TO _____	1986 January 31	20

16. SUPPLEMENTARY NOTATION *Northeastern University, Boston, MA 02115

This work is supported by the Defense Advanced Research Projects Agency under Contract No. 5483.

17. COSATI CODES			18. SUBJECT TERMS (Continue on reverse if necessary and identify by block number)
FIELD	GROUP	SUB-GROUP	Electron cyclotron maser Induced resonance electron-cyclotron ~~(IREC)~~ quasi-optical maser

19. ABSTRACT (Continue on reverse if necessary and identify by block number)

In this paper we analyze an induced resonance electron cyclotron (IREC) quasi-optical maser configuration. This configuration has the unique features of being highly efficient and at the same time relatively insensitive to the detrimental effects of poor beam quality. A system of nonlinear coupled orbit equations, describing the dynamics of electrons in a spatially varying external magnetic field and the electromagnetic field of a steady state oscillator, are derived and analyzed. We show that with the proper choice for the index of refraction, the high frequency cyclotron interaction can be made insensitive to a beam energy spread. The interaction can, however, be sensitive to the beam's pitch angle spread. The necessary conditions on beam quality for high efficiency operation are derived and shown to be in good agreement with our numerical solutions. Furthermore, we show that by appropriately tapering the magnetic field an induced resonance condition can be achieved which results in high interaction efficiencies. It is anticipated that an efficient, high power millimeter, submillimeter and infrared radiation source can be realized with the IREC quasi-optical maser configuration.

20. DISTRIBUTION / AVAILABILITY OF ABSTRACT	21. ABSTRACT SECURITY CLASSIFICATION
☒ UNCLASSIFIED/UNLIMITED ☐ SAME AS RPT. ☐ DTIC USERS	UNCLASSIFIED
22a. NAME OF RESPONSIBLE INDIVIDUAL P. Sprangle	22b. TELEPHONE (Include Area Code) (202) 767-3493 22c. OFFICE SYMBOL Code 4790

DD FORM 1473, 84 MAR 83 APR edition may be used until exhausted. All other editions are obsolete.

SECURITY CLASSIFICATION OF THIS PAGE

CONTENTS

INDUCED RESONANCE ELECTRON CYCLOTRON (IREC) QUASI-OPTICAL MASER

Introduction

This paper deals with a variation of an electron cyclotron interaction which may, because of its unique features, find applications as a powerful and efficient short wavelength radiation source. In general, an electron cyclotron maser interaction takes place when a resonance exists between an electron's cyclotron motion and the Doppler-shifted electromagnetic wave frequency. One class of electron cyclotron interactions was proposed independently in the late 1950's by a number of researchers[1-4] and is the basis of the electron cyclotron maser radiation source (gyrotron).[5-25] Typically, in gyrotrons, the electrons are mildly relativistic and the interaction frequency is low, approximately equal to the electron's cyclotron frequency. In the gyrotron mechanism, the electrons experience primarily azimuthal bunching resulting in an induced current density which drives the radiation field. The gyrotron process is also generally believed to be responsible for radiation observed from the earth's magnetic poles,[26,27] solar atmosphere[28-30] and tandem mirror devices.[31] Electromagnetic cyclotron interactions have also been proposed as potential laser driven acceleration mechanisms[32,33] as well as a possible mechanism responsible for high energy electrons observed in type III solar burst.[34]

In this paper we analyze an induced resonance electron cyclotron (IREC) quasi-optical maser. Here the beam electrons are highly relativistic and the interaction frequency is much greater than the electron cyclotron frequency. The intrinsic efficiency is found to be insensitive to the electron's energy. In this high frequency electron cyclotron interaction, the transverse

Manuscript approved October 28, 1985.

as well as the longitudinal beam energy is converted into radiation. This is unlike the usual gyrotron interaction in which primarily transverse energy is converted to radiation. By spatially tapering the external magnetic field an induced resonance condition can be achieved which is shown to substantially enhance the overall operating efficiency. The effects of finite electron beam quality, fractional energy and pitch angle spread, can be minimized.

The IREC maser mechanism is similar to that of the cyclotron autoresonance maser (CARM).[17,21,24] There are, however, a number of important differences. In the present mechanism the magnetic field is tapered to provide induced resonance. The radiation refractive index is chosen to minimize the effects of finite beam quality, and the number of electron cyclotron orbits within the interaction length is kept small, i.e., typically less than ten. Furthermore, the interaction takes place within an open resonator.

We derive a set of one-dimensional, fully nonlinear and relativistic orbit equations for particles in a radiation field and spatially tapered static magnetic field. These equations are used to study a high frequency electron cyclotron interaction within a steady state oscillator configuration. In our oscillator model we assume a large amplitude temporally steady state radiation field within a resonator. Electrons are injected into the oscillator along a static magnetic field with a longitudinal velocity (parallel to $\underline{B}_o$) much larger than their gyrational (transverse) velocity. The electrons enter the oscillator uniformly distributed in both phase and position. Under the appropriate conditions the average electron energy flux (power) will be less at the output of the oscillator than at the input. Assuming an ideal resonator, i.e., no diffraction or ohmic losses, the average change in electron energy flux in the steady state just equals the output radiation power of the oscillator.

Fields and Particle Dynamics

To analyze the behavior of the IREC quasi-optical maser we employ a simplified model which consists of a gyrating electron beam streaming along a nonuniform static magnetic field. The electron beam is propagated through a plane-parallel plate resonator containing a large amplitude steady state radiation field as shown in Fig. 1a. The vector potential associated with the radiation field within the resonator is a circularly polarized standing wave of the form

$$\underline{A}(z,t) = 2A \sin (k_\ell z) (\cos (\omega_\ell t)\hat{e}_x + \sin (\omega_\ell t)\hat{e}_y), \tag{1}$$

where A is the constant amplitude, $k_\ell = 2\pi\ell/L$ is the longitudinal wave number, $\omega_\ell = c(k_\ell^2 + k_\perp^2)^{1/2}$ is the frequency, $k_\perp << k_\ell$ is the transverse wave number, ℓ is a positive integer denoting the number of half wavelengths within the resonator and L is the resonator length. The external nonuniform static magnetic field is

$$\underline{B}_o(x,y,z) = - (1/2)(x\hat{e}_x + y\hat{e}_y)\partial B_o(z)/\partial z + B_o(z)\hat{e}_z, \tag{2}$$

where $B_o(z)$ is the slowly varying longitudinal component of field. Since we are interested in the high frequency interaction of the gyrating beam with the radiation we considered only the forward propagating component of the field in (1) which is

$$\underline{A}_+(z,t) = A(\sin \Phi_\ell(z,t)\hat{e}_x + \cos \Phi_\ell(z,t)\hat{e}_y), \tag{3}$$

where $\Phi_\ell = k_\ell z - \omega_\ell t$. To obtain the fully nonlinear and relativistic particle orbits we denote the transverse position and momentum of a particle by

$$x = x_g + r \sin\Theta, \qquad y = y_g - r\cos\Theta, \tag{4a,b}$$

$$P_x = p_{gx} + P_\perp \cos\Theta, \qquad P_y = P_{gy} + P_\perp \sin\Theta, \tag{4c,d}$$

respectively. In this representation (x_g, y_g) and (P_{gx}, P_{gy}) denote the transverse coordinates and momentum of the particle's guiding center, r is the Larmor radius, $P_\perp$ is the magnitude of the transverse momentum and Θ is the momentum space angle. We assume that x_g, y_g, P_{gx}, P_{gy} r, $P_\perp$ and $\psi = \Theta + \Phi_\ell$ are slowly varying functions of z, i.e., change little during a gyro period. Using the Lorentz force equation together with the fields in (2) and (3) and the particle orbit representation in (4), the nonlinear particle orbit equations for $P_\perp$, P_z and ψ can be cast into the following form

$$\frac{\partial U_\perp}{\partial z} = -\, a\,\frac{\omega}{c}\,\frac{(\gamma - nU_z)}{U_z}\cos\psi + \frac{U_\perp}{2}\,B_o^{-1}\,\frac{\partial B_o}{\partial z}, \tag{5a}$$

$$\frac{\partial U_z}{\partial z} = -\, an\,\frac{\omega}{c}\,\frac{U_\perp}{U_z}\cos\psi - \frac{U_\perp^2}{2U_z}\,B_o^{-1}\,\frac{\partial B_o}{\partial z}, \tag{5b}$$

$$\frac{\partial \psi}{\partial z} = -\,\Delta\omega/c + a\,\frac{\omega}{c}\,\frac{(\gamma - nU_z)}{U_\perp U_z}\sin\psi, \tag{5c}$$

where $U_\perp = P_\perp/m_o c$, $U_z = P_z/m_o c$, $\gamma = (1 + U_\perp^2 + U_z^2)^{1/2}$ is the relativistic mass factor, $a = |e|A_+/m_o c^2$ is the normalized radiation amplitude, $\psi = \Theta + \Phi$ is the relative phase between the radiation field and particle, $n = ck/\omega = 1 - (k_\perp/k)^2/2$ is the refractive index associated with the radiation field $\Delta\omega = (\omega(1 - n\beta_z) - \Omega_o/\gamma)/\beta_z$ is the frequency mismatch term and $\Omega_o = |e|B_o/m_o c$ is the electron cyclotron frequency. The frequency mismatch term $\Delta\omega$ will be shown to play a central role in the cyclotron interaction. The subscript ℓ denoting the mode number

has been omitted from the frequency and wave number. Using (5a) and (5b) the spatial rate of change of γ is given by

$$\frac{\partial \gamma}{\partial z} = - a \frac{\omega}{c} \frac{U_\perp}{U_z} \cos \psi. \tag{6}$$

Equations (5a,b,c) are the nonlinear orbit equations for a single particle in the tapered external magnetic field given by (2) interacting with a forward going resonator field given by (3).

The interaction frequency is determined by the resonant frequency condition, $\omega - v_{oz} k - \Omega_o/\gamma_o = \beta_{oz}\Delta\omega_o$, and the eigenfrequency of the resonator $\omega = ck(1 + (k_\perp/k)^2/2)$. The simultaneous solution of these equations yield the interaction frequency

$$\omega = (1 + \beta_{oz})\gamma_{oz}^2 \frac{(\Omega_o/\gamma_o + \beta_{oz}\Delta\omega_o)}{1 + \beta_{oz}(1 + \beta_{oz})\gamma_{oz}^2\varepsilon} \approx 2\gamma_{oz}^2 \Omega_o/\gamma_o, \tag{7}$$

where $\varepsilon = 1-n = (k_\perp/k)^2/2$ and the last expression in (7) assumes $\beta_{oz} \approx 1$, $|\Delta\omega_o| << \Omega_o/\gamma_o$ and $|\varepsilon| << 1/2\gamma_{oz}^2$. Note that this is similar to the conventional free electron laser,[35] where the interaction frequency is given by $\omega = 2\gamma_{oz}^2 ck_w$ where k_w is the wiggler wave number.

Before considering the effect of a spatially contoured external magnetic field on the interaction we first consider the case where B_o is constant. For B_o constant the orbit equations in (5) process two constants of motion which are

$$U_z - n\gamma = C_1, \tag{8a}$$

$$U_\perp^2 - 2\Omega_o\gamma/\omega - 2aU_\perp \sin \psi = C_2. \tag{8b}$$

With the use of the constant of motion C_1 it is possible to estimate the change in electron energy necessary to produce a change in ψ equal to π. This energy change is expected to yield an estimate for the maximum energy change an electron can undergo within the resonator. To this end we expand the $\Delta\omega$ term in the phase equation (5c) about its initial value $\Delta\omega_o$, writing $\Delta\omega = \Delta\omega_o + (\partial\Delta\omega/\partial\gamma)_o(\gamma - \gamma_o)$ where the subscript o denotes the value at $z = 0$ and using (8a) we find that $(\partial\Delta\omega/\partial\gamma)_o = (\omega(1 - n^2) - n\Delta\omega_o)/U_{oz}$. Since $\omega = (\Omega_o + U_{oz}\Delta\omega_o)/(\gamma_o - nU_{oz})$, $(\partial\Delta\omega/\partial\gamma)_o$ becomes

$$\left(\frac{\partial\Delta\omega}{\partial\gamma}\right)_o = \frac{\Omega_o}{\gamma_o}\,\frac{\left(1 - n^2 + \gamma_o(\beta_{oz} - n)\Delta\omega_o/\Omega_o\right)}{(1 - n\beta_{oz})\,\beta_{oz}\gamma_o}. \tag{9}$$

The maximum change in electron energy at the end of the resonator, $z = L$, is found by setting $(\partial\Delta\omega/\partial\gamma)_o\,(\gamma - \gamma_o)L/c$ equal to $\approx \pi$ giving

$$\left|\frac{\gamma - \gamma_o}{\gamma_o}\right| \approx \frac{1}{2N_c}\left|\frac{(1 - n\beta_{oz})}{\left(1 - n^2 + \frac{\gamma_o\Delta\omega_o}{\Omega_o}(\beta_{oz} - n)\right)}\right| \approx \frac{1}{2N_c}\left|\frac{(1 - n\beta_{oz})}{(1 - n^2)}\right| \approx \frac{\omega\Omega_o/\gamma_o}{c^2k_\perp^2}, \tag{10}$$

where $N_c = \Omega_o L/(2\pi\gamma_o v_{oz})$ is the number of electron cyclotron orbits within the resonator. The last inequality in (8) assumes $|\Delta\omega_o|$ is small compared to $|\Omega_o(1 - n^2)/\gamma_o(\beta_{oz} - n)|$. Equation (8) may be used to obtain an estimate for the interaction efficiency. Although N_c may be large, say on the order of 10, the term $(1 - n\beta_{oz})/(1 - n^2)$ can be chosen, within certain limits, to be large resulting in high interaction efficiencies. By spatially tapering the applied magnetic field the cyclotron resonance condition can be further extended (induced resonance) resulting in higher efficiencies. The similarity between (10) and the low gain estimate for efficiency in the free electron laser[35] is apparent. In the low gain FEL the intrinsic (untapered wiggler) efficiency is $1/2N_w$ where N_w is the number of wiggler periods within the interaction region.

Effect of Input Beam Quality

Another important property of the IREC maser is, if the refractive index n is appropriately chosen, its insensitivity to a spread in the beam electrons longitudinal velocity. The effect of an electron velocity spread is manifested by a spread in the frequency mismatch term $\Delta\omega$. The velocity spreads associated with the input beam electrons must be kept small enough so that the frequency mismatch spread does not lead to a significant spread in the electron phase ψ. The condition necessary to insure that the spread in ψ at the end of the resonator is much less than π is

$$\left| \left(\frac{\partial \Delta\omega}{\partial v_z}\right) \delta v_z + \left(\frac{\partial \Delta\omega}{\partial v_\perp}\right) \delta v_\perp \right| \frac{L}{c} \ll \pi, \tag{11}$$

where δv_z and $\delta v_\perp$ denote the thermal spread in longitudinal and transverse electron velocity about v_{oz} and $v_{o_\perp}$ respectively. Using the definition of $\Delta\omega$, the inequality in (11) becomes

$$\left| (\gamma_o \Omega_o \beta_{oz} - n\omega - \Delta\omega_o) \delta v_z + \gamma_o \Omega_o \beta_{o_\perp} \delta v_\perp \right| \ll \frac{\pi v_{oz} c}{L}. \tag{12}$$

Since $|\Delta\omega_o| \ll \gamma_o \Omega_o \beta_{oz}$ or $n\omega$, the coefficient of the δv_z term in (12) can be neglected if the index of refraction is

$$n \approx \gamma_o \Omega_o \beta_{oz} / \omega. \tag{13}$$

With this choice of n the inequality in (12) becomes

$$\left| \delta\beta_\perp \right| \ll \frac{1}{2N_c \beta_{o_\perp} \gamma_o^2}. \tag{14}$$

It proves convenient to measure beam quality in terms of $\Delta\gamma/\gamma_o$ and $\Delta\theta/\theta_o$; the fractional half-width average spread in the relativistic mass factor and the velocity pitch angle $\theta_o = \beta_{o\perp}/\beta_{oz}$. The quantities $\Delta\gamma/\gamma_o$ and $\Delta\theta/\theta_o$ are positive and assumed small. In terms of $\Delta\gamma/\gamma_o$ and $\Delta\theta/\theta_o$ the average transverse beam velocity spread is $\Delta\beta_\perp = \theta_o(\Delta\gamma/\gamma_o + \gamma_o^2\Delta\theta/\theta_o)/\gamma_o^2$ which replaces $|\delta\beta_\perp|$ in (14) giving

$$\Delta\theta/\theta_o + \gamma_o^{-2}\Delta\gamma/\gamma_o << \frac{\beta_{oz}}{2N_c\beta_{o\perp}^2\gamma_o^2}. \tag{15}$$

If the inequality in (15) is satisfied, the beam's finite spread in pitch angle and energy will have little effect on the interaction. For highly relativistic electron beams the inequality in (15) demonstrates that a beam pitch angle spread is more detrimental to the interaction than a beam energy spread. This point will be further demonstrated later.

The interaction frequency is $\omega = v_{oz}k + \Omega_o/\gamma_o + \beta_{oz}\Delta\omega_o$ which upon using the index of refraction in (13) and neglecting $\Delta\omega$ gives

$$\omega = \gamma_o\Omega_o(1 - \beta_{o\perp}^2). \tag{16}$$

To achieve a high frequency interaction and reduce the effect of an electron pitch angle spread, see Eq. (15), it is necessary to have $\beta_{o\perp}^2 << 1$.

Discussion and Numerical Results

In this paper we are primarily interested in utilizing the high frequency interaction in an oscillator configuration to generate high power levels of millimeter, submillimeter and infrared radiation efficiently. To this end the particle equations in (5) are numerically integrated for an ensemble of particles and the average electron energy flux change is obtained. Our analysis is based on the idealized model shown in Fig. 1a, but perhaps a more practical configuration for this mechanism is that shown in Fig. 1b. In Fig. 1b both the electron beam and tapered magnetic field are directed at an angle to the resonator's axis. The purpose of the tapered magnetic field is to prolong the resonance condition for the average electron and hence enhance efficiency.

Figure 2 shows the efficiency (average change in electron beam energy flux in passing through the resonator/input beam energy flux) as a function of axial distance measured in terms of electron cyclotron orbits for a particular set of parameters. The parameters for this figure are $\gamma_o = 4$, $\beta_{o\perp} = 1/\gamma_o = 0.25$, $\beta_{oz}\,\Delta\omega_o/\Omega_o = 0.035$, $n = 0.9885$ and $a = |e|A/m_o c^2 = 0.025$. Curve (a) is obtained from a small signal analysis of the orbit equations.[36] Curve (b) is obtained by numerically integrating the orbit equations for an ensemble of electrons in a uniform magnetic field. For this curve the maximum intrinsic efficiency is ~ 15% and is reached after ~ 5 cyclotron orbits. Curve (c) shows the efficiency when the external magnetic field is tapered. For this curve the magnetic field is held constant until the electrons phase bunch. At this point induced resonance is achieved by linearly increasing the magnetic field by ~ 35% and the maximum enhanced efficiency is ~ 44%. This particular spatial magnetic field variation is not optimum, but was chosen simply as an illustration. Comparing curves (b) and (c) we see that by tapering the

magnetic field the peak efficiency is increased by a factor of three over the uniform field case. Tapering the magnetic field, however, increases the number of cyclotron orbits needed to reach the peak efficiency ($N_c \approx 11$).

Figure 3 shows the peak efficiency vs. normalized radiation field amplitude for various values of the frequency mismatch parameter. In this figure $\gamma_o = 4$, $\beta_{o\perp} = 1/\gamma_o = 0.25$ and the number of electron cyclotron orbits at maximum efficiency and the index of refraction are for curve (a) $N_c \approx 20$, $n = 0.9950$, for curve (b) $N_c \approx 10$, $n = 0.9925$, for curve (c) $N_c \approx 5$, $n = 0.9885$ and for curve (d) $N_c \approx 3.5$, $n = 0.9849$. As the frequency mismatch parameter $\beta_{oz}\, \Delta\omega_o/\Omega_o$ is decreased, both the peak efficiency as well as the number of electron cyclotron orbits necessary to achieve the peak efficiency increases. Although this mechanism is insensitive to a beam energy spread if the index of refraction is $n = \gamma_o \Omega_o \beta_{oz}/\omega$, Eq. (13), it can be sensitive to a pitch angle spread, see Eq. (15). For the parameters chosen in Fig. 3, the beam's pitch angle spread must satisfy $\Delta\theta/\theta_o \ll 1/2N_c$.

Figure 4 shows the effect on efficiency when the injected beam has either a spread in pitch angle or a spread in energy. In this figure the parameters are the same as those corresponding to the peak efficiency ($\eta \approx 44\%$) in curve (c) of Fig. 2. In Fig. 4 the cold beam efficiency is reduced by 50% by a half-width beam pitch angle spread of $\sim 4\%$ or by a half-width beam energy spread of 22%. In this figure the number of cyclotron orbits needed to reach peak efficiency was large, $N_c \approx 11$.

ACKNOWLEDGMENTS

This work is sponsored by DARPA under Contract Number 5483.

INDUCED RESONANCE ELECTRON CYCLOTRON (IREC)

QUASI-OPTICAL MASER

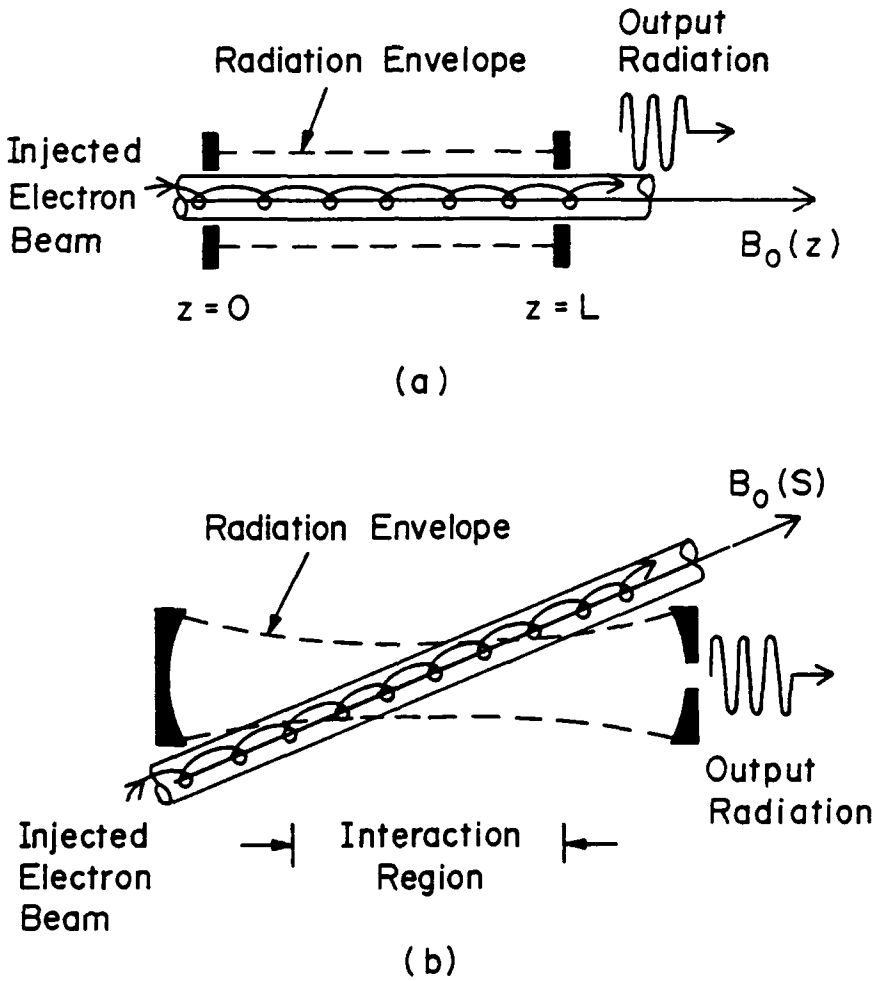

Fig. 1 — Shows the high freguency electron cyclotron maser configuration (a) an idealized model consisting of a parallel-plate resonator and electron beam. The individual electrons stream along and gyrate about a tapered magnetic field, (b) here a more realistic model consists of an open resonator in which both the magnetic field and electron beam are directed at an angle to the resonator's axis.

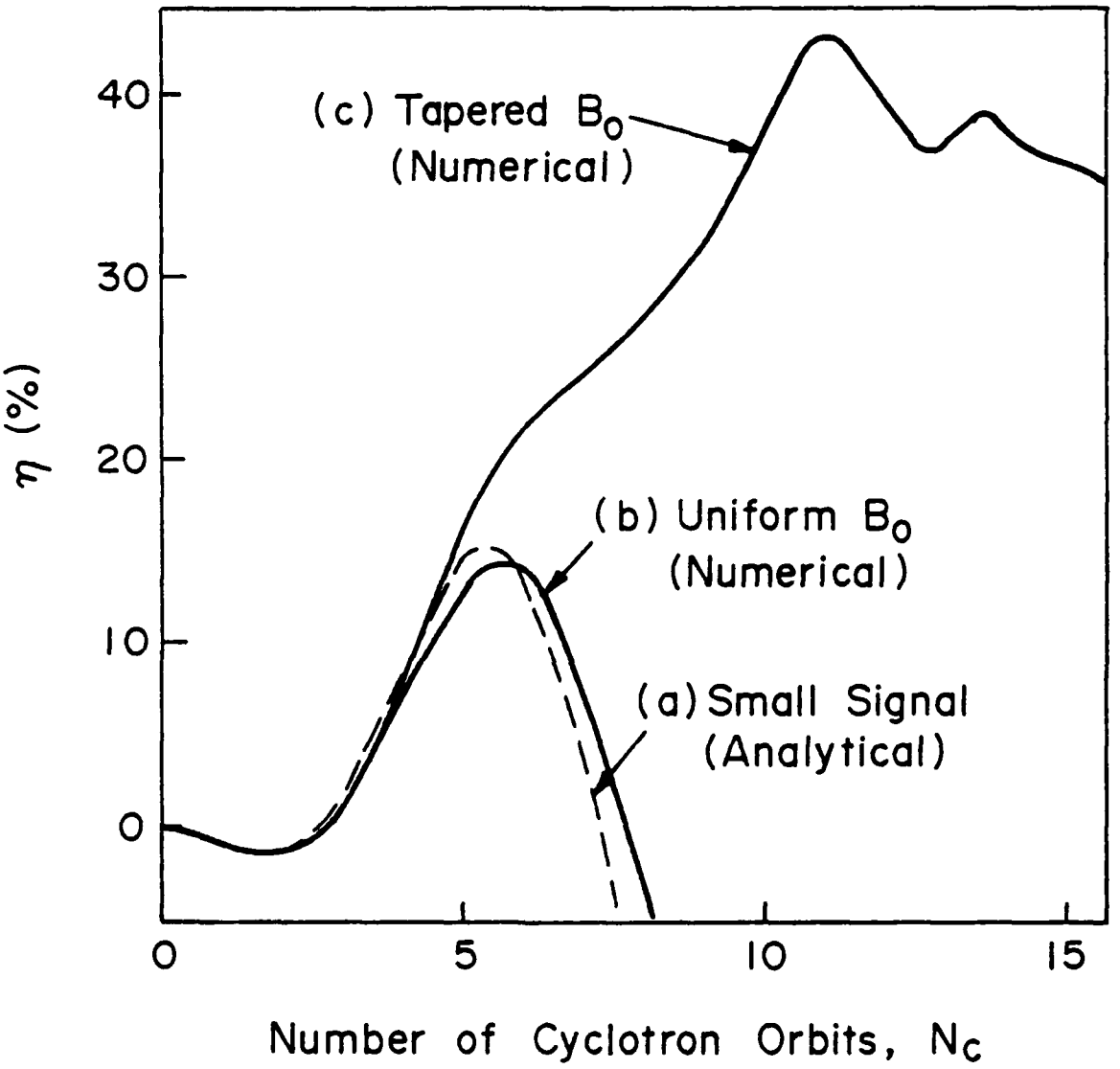

Fig. 2 — Shows the efficiency as a function of axial distance measured in terms of electron cyclotron orbit. Curve (a) is obtained from a small signal analysis, curve (b) is for a uniform magnetic field and curve (c) is for a spatially tapered magnetic field.

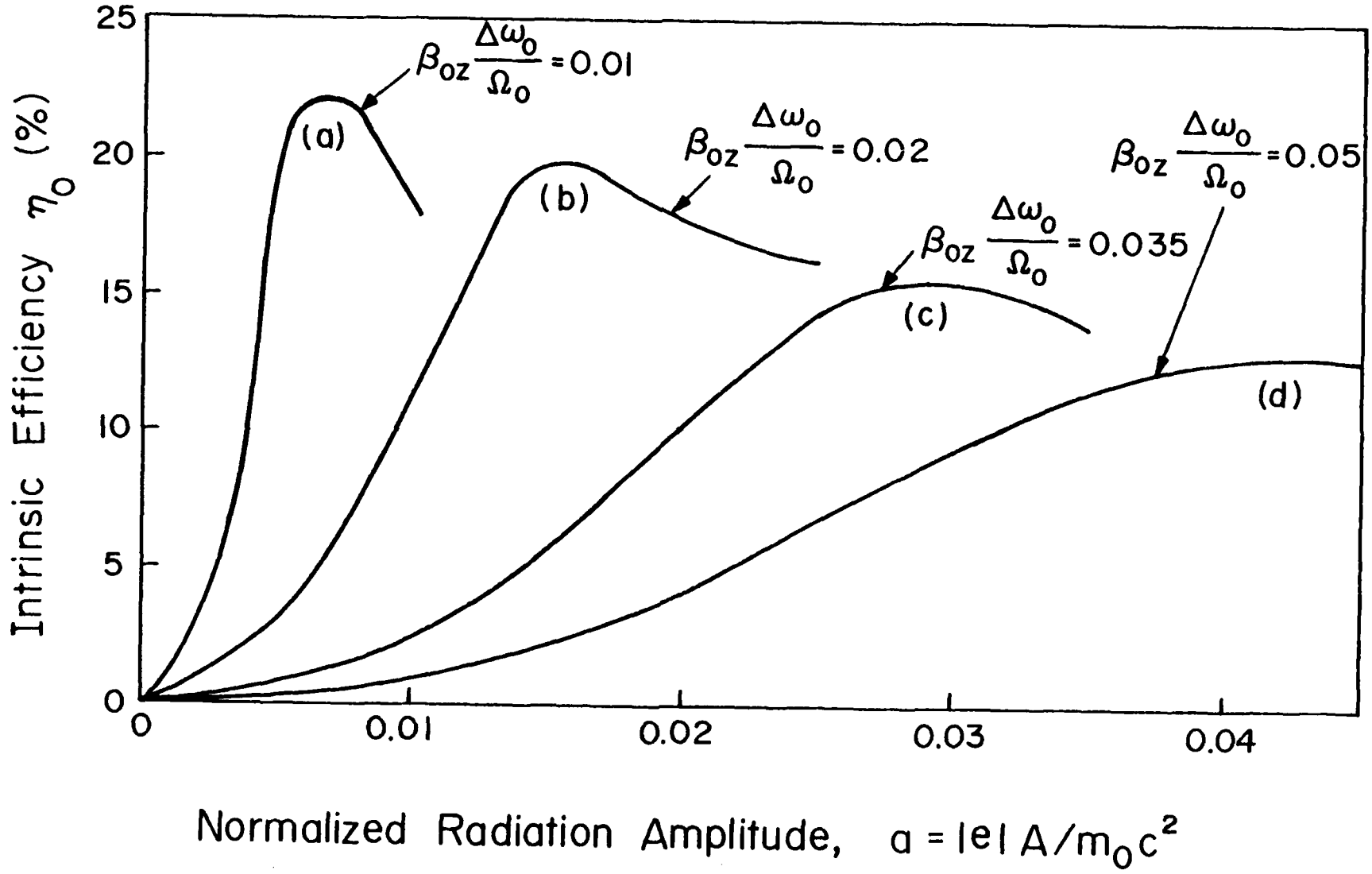

Fig. 3 — Shows the peak efficiency as a function of the radiation amplitude for various values of the frequency mismatch parameter. The normalized frequency mismatch $\beta_{oz}\ \Delta\omega_0/\Omega_0$ is shown for each curve.

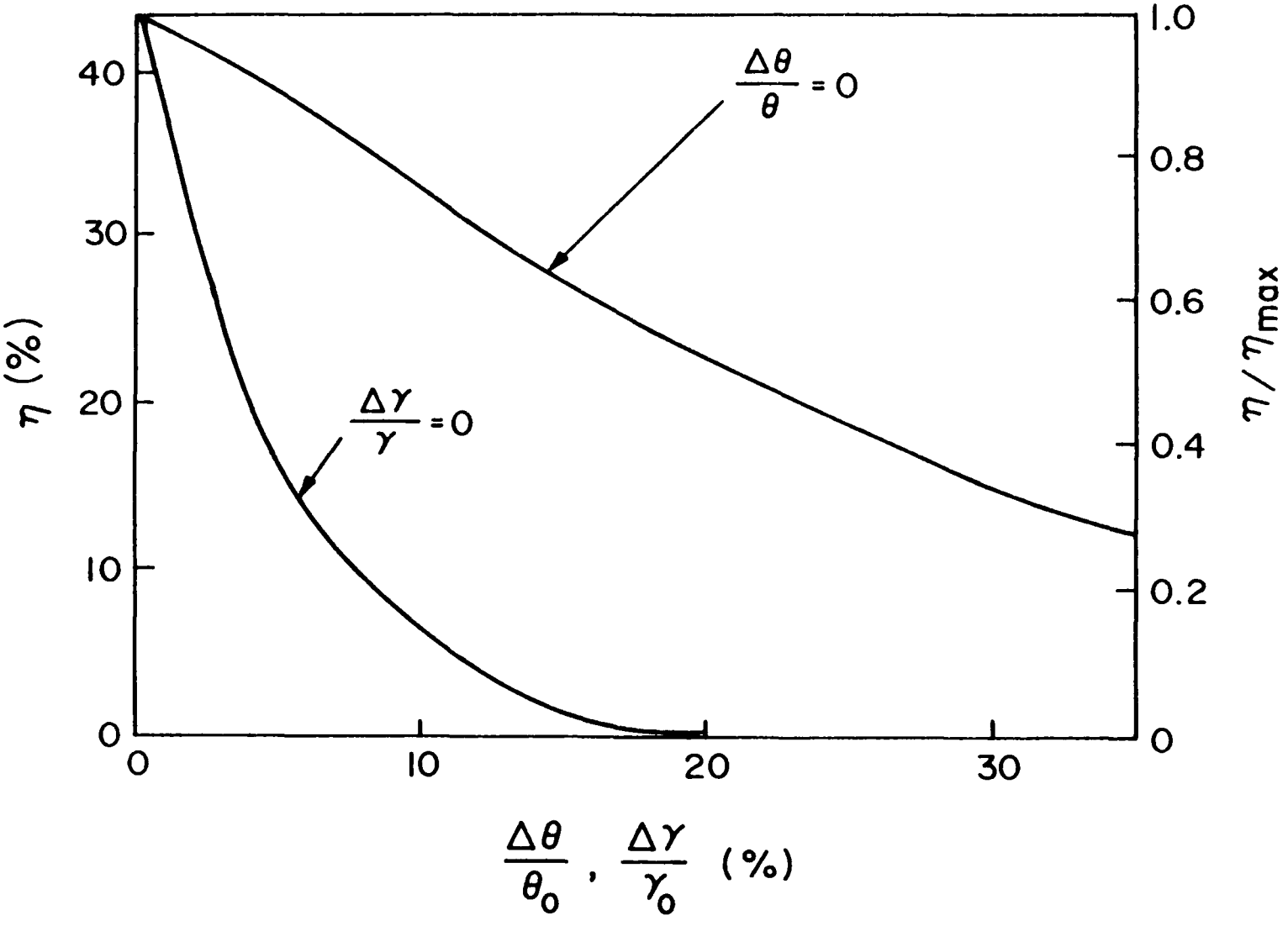

Fig. 4 — Shows the efficiency fall-off for beams with a pitch angle spread or energy spread. In this figure the magnetic field is tapered and the peak efficiency is 44% for $\Delta\theta/\theta_0 = \Delta\gamma/\gamma_0 = 0$.

REFERENCES

1. R. Q. Twiss, Aust. J. Phys., 11, 564, (1958).

2. A. V. Gaponov, Isv. Vyssh. Uchebn, Zaved, Radiofiz., 2, 450, (1959).

3. R. H. Pantell, Proc. IRE, 47, 1146, (1959).

4. J. Schneider, Phys. Rev. Lett. 2, 504 (1959).

5. J. L. Hirshfield and J. M. Wachtel, Phys. Rev. Lett. 12, 533 (1964).

6. A. V. Gaponov, M. I. Petelin and V. K. Yulpalov, Radio Phys. Quantum Electron. 110, 94 (1967).

7. V. L. Bratman, M. A. Moiseev, M. I. Petelin and R. E. Erm, Radio Phys. Quantum Electron. 16, 474 (1973).

8. D. V. Kisel', G. S. Korablev, V. G. Navel'yev, M. I. Petelin and Sh. E. Tsimring, Radio Eng. Electron. Phys. 19, No. 4, 95 (1974).

9. N. I. Zaytsev, T. B. Pankratova, M. I. Petelin and V. A. Flyagin, Radio Eng. Electron. Phys. 19, No. 5 103 (1974).

10. V. L. Granatstein, M. Herndon, R. K. Parker and P. Sprangle, IEEE J. Quantum Electron. QE-10 No. 9 p. 651 (1974).

11. E. Ott and W. M. Manheimer, IEEE Trans. Plasma Science PS-3, 1 (1975).

12. V. L. Granatstein, P. Sprangle, M. Herndon and R. K. Parker, J. Appl. Phys. 46, 2021 (1975).

13. P. Sprangle and W. M. Manheimer, Phys. Fluids 18, 224 (1975).

14. P. Sprangle and A. T. Drobot, IEEE Trans. Microwave Theory and Techniques MTT-25, 528 (1977).

15. J. L. Hirshfield and V. L. Granatstein, IEEE Trans. Microwave Theory and Tech. MTT-25, 522 (1977).

16. K. R. Chu and J. L. Hirshfield, Phys. Fluids 21, 461, (1978).

17. V. L. Bratman, N. S. Ginzburg and M. I. Petelin, Optics Commun. 30, 409 (1979).

18. P. Sprangle and R. A. Smith, J. Appl. Phys. 51, 6, p. 3001 (1980).

19. P. Sprangle, J. L. Vomvoridis and W. M. Manheimer, Appl. Phys. Lett. 38, 5, p. 310 (1981), also Phys. Rev. A23, 3127, (1981).

20. K. E. Kreischer and R. J. Temkin, Intl. J. of Infrared and Millimeter Waves, Vol. 2, No. 2 p. 175 (1981).

21. V. L. Bratman, N. S. Ginzburg, G. S. Nusinovich, M. I. Petelin and P. S. Strelkow, Intl. J. Electron. 51, 541 (1981).

22. I. E. Botvinnik, V.L. Bratman, A. B. Volkov, N. S. Ginzburg, G. G. Denisov, B. D. Kol'chugin, M. N. Ofitserov and M. I. Petelin, JETP Lett., Vol. 35, No. 10, pp. 516, (1982).

23. Y Y. Lau, IEEE Trans., Vol. ED-29, No. 2, pp. 320, (1982).

24. V. L. Bratman, G. G. Denisov, N. S. Ginzburg and M. I. Petelin, IEEE J. Quantum Electron, Vol. QE-19, No. 3, (1983).

25. A. T. Lin, W. W. Chang and C. C. Lin, Phys. Fluids 27, 1054 (1984).

26. C. S. Wu and L. C. Lee, Astrophysical Journal 230, 621 (1979).

27. H. P. Freund, H. K. Wong, C. S. Wu and M. J. Xu, Phys. Fluids 26, 2263 (1983).

28. R. R. Sharma, L. Vlahos and K. Papadopoulos, Astronomy and Astrophysics 112, 377 (1982).

29. D. B. Melrose and G. A. Dulk, Astrophysical Journal 259, 844 (1982).

30. L. Vlahos and P. Sprangle, Univ. of Md. Memo Report No. AP85-039, also submitted to Astrophysical Journal (1984).

31. Y. Y. Lau and K. R. Chu, Phys. Rev. Lett., 50, 243, (1983).

32. A. A. Kolomenskii and A. N. Lebedev, Dok. Akad. Nauk. SSSR 145, 1259 (1962) and Sov. Phys. Dokl. 7, 745 (1963).

33. P. Sprangle, L. Vlahos and C. M. Tang, IEEE Trans. Nucl. Sci. NS-30, 3177 (1983).

34. P. Sprangle and L. Vlahos, Astrophysical Journal (Letters) 273, L95 (1983).

35. Free-Electron Generators of Coherent Radiation, Phys. of Quantum Electronics, S. F. Jacobs, H. S. Pilloff, M. Sargent III, M. O. Scully, R. Spitzer, eds. Addison-Wesley, Reading, Mass. (1980) Vols. 7, 8 and 9.

36. J. L. Vomvoridis and P. Sprangle, Phys. Rev. A25, 931 (1982).

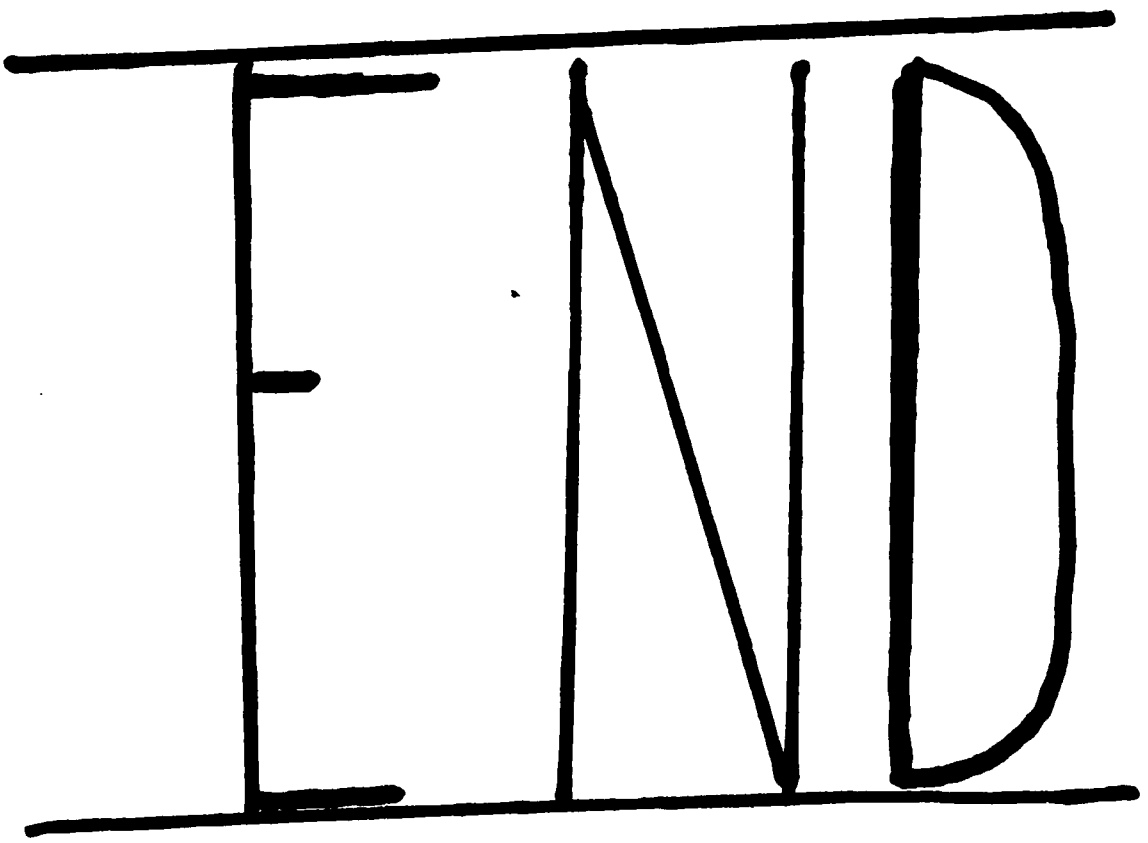

FILMED

3

-86

DTIC